IDO-16611

EFFECTS OF GAMMA RADIATION ON REACTIVITY MEASUREMENTS IN THE REACTIVITY MEASUREMENT FACILITY

D. G. Proctor
G. K. Wachs

April 28, 1961

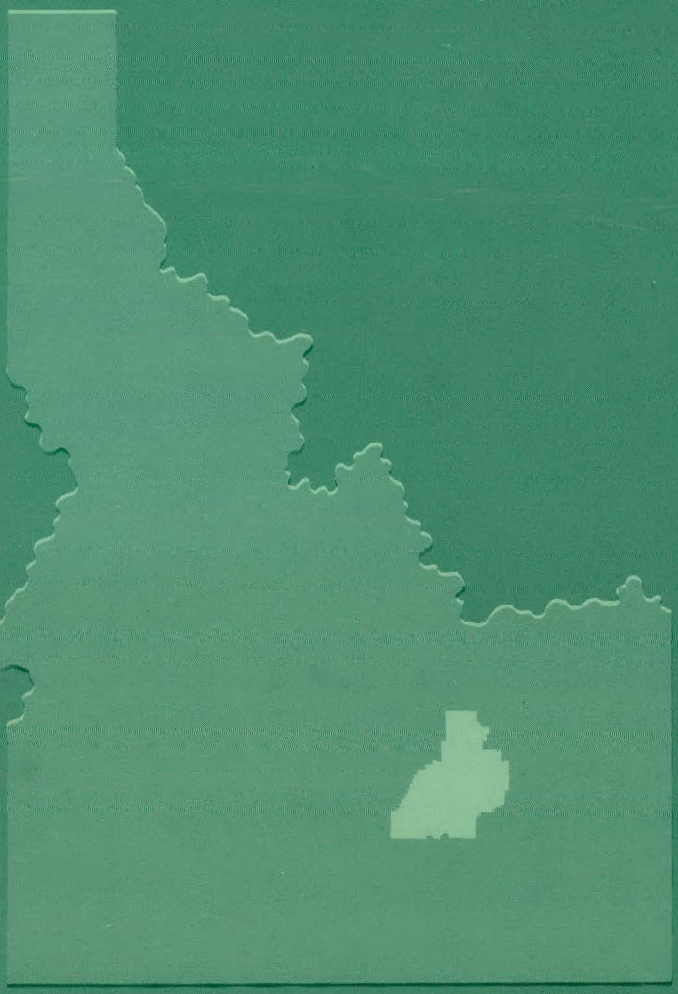

PHILLIPS PETROLEUM COMPANY

ATOMIC ENERGY DIVISION

NATIONAL REACTOR TESTING STATION
US ATOMIC ENERGY COMMISSION

DISCLAIMER

PRICE $ .75

Available from the
Office of Technical Services
U. S. Department of Commerce
Washington 25, D. C.

Printed in USA

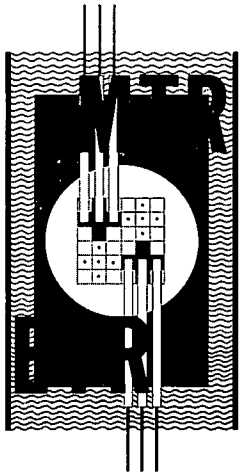

MATERIALS TESTING REACTOR
ENGINEERING TEST REACTOR

IDO-16611
AEC Research and Development Report
Reactor Technology
TID-4500 (16th Ed.)
Issued: April 28, 1961

EFFECTS OF GAMMA RADIATION ON REACTIVITY MEASUREMENTS IN THE REACTIVITY MEASUREMENT FACILITY

D. G. Proctor and G. K. Wachs

PHILLIPS
PETROLEUM
COMPANY

Atomic Energy Division
Contract AT(10-1)-205
Idaho Operations Office
U. S. ATOMIC ENERGY COMMISSION

THIS PAGE

WAS INTENTIONALLY

LEFT BLANK

EFFECTS OF GAMMA RADIATION ON REACTIVITY MEASUREMENTS IN THE REACTIVITY MEASUREMENT FACILITY

by

D. G. Proctor and G. K. Wachs

A B S T R A C T

The effect of gamma radiation from radioactive samples measured in the RMF has been studied. No detectable effect due to photoneutrons was found when irradiated fuel samples were used as samples. Also no measurable reactivity effect was found when a decaying gamma-ray source was used as a test sample. A method of estimating the reactivity error due to a decaying gamma-ray source is described. A comparison between geometrically-compensated and electrically-compensated ion chambers is made which shows that the electrically-compensated ion chamber is better suited for use in the RMF.

THIS PAGE

WAS INTENTIONALLY

LEFT BLANK

TABLE OF CONTENTS

LIST OF TABLES

LIST OF FIGURES

EFFECTS OF GAMMA RADIATION ON REACTIVITY MEASUREMENTS IN THE REACTIVITY MEASUREMENT FACILITY

by

D. G. Proctor and G. K. Wachs

I. INTRODUCTION

Because the sensitivity of the Reactivity Measurement Facility is high, small effects due to radioactivity of test samples can possibly be seen. The magnitude of these effects could be high enough to contribute significant errors to the burnup studies of fuel samples whose reactivity changes are measured while the level of gamma radiation is very high. This report discusses tests performed to determine whether or not gamma radiation effects can be seen and if so, to determine the magnitude of the effects.

The two effects studied are: 1) photoneutron production and 2) reactivity changes due to lack of compensation in the servo control chamber. In connection with the gamma-ray compensation problem, a comparison was made between two types of compensated ion chambers to determine which type is more suitable for control purposes in the Reactivity Measurement Facility.

Although these experiments are by no means extensive, they show at what point gamma radiation may be expected to become bothersome. More extensive studies will be necessary if the gamma radiation levels are higher than indicated in these tests.

II. EFFECT OF PHOTONEUTRONS ON THE RMF

Reactivity measurements are sometime made with irradiated samples soon after being exposed to the high neutron flux levels present in the MTR. An example is the determination of reactivity changes associated with fission product transient experiments. The samples for these experiments contain fissionable materials which during irradiation produce fission products emitting highly intense gamma radiation with some gamma rays energetic enough to produce photoneutrons. The fission product gamma rays mainly responsible for photoneutron production are the 2.5 Mev La^{140}, 2.4 Mev I^{135} and 2.6 Mev Pr^{144} gamma rays.[1] These gamma rays are sufficiently energetic to produce photoneutrons from the deuterium normally present in the ordinary water used as the moderator and reflector in the RMF. Photoneutrons produced by the (γ,n) reaction appear to the reactor as a source,

1. John Moteff, "Fission Product Decay Gamma Energy Spectrum", Aircraft Nuclear Propulsion Project, General Electric, Cincinnati, Ohio, APEX-134, June 1953.

thus changing the regulating rod position necessary to maintain criticality. Therefore the measured reactivity of a sample will change. As a result, the comparison of measured reactivities of an irradiated sample to an identical unirradiated sample will not be valid. These errors could be significant in comparing reactivities for the fission product transient experiment. Consequently this experiment was conducted using a typical irradiated sample to investigate the effect of photoneutrons on reactivity measurements.

Measurement of the effect of photoneutrons may be accomplished by operating the reactor at two different power levels. A derivation showing the effect of photoneutrons on reactivity measurements follows:

The differential equation for the neutron density is

$$\frac{dn}{dt} = S + \frac{n(k_{ex} - \beta)}{\ell^*} + \sum_i \lambda_i C_i , \qquad (1)$$

where

n = neutron density,

$\frac{dn}{dt}$ = time rate of change of the neutron density,

S = source term, in this case due to the photoneutrons,

k_{ex} = excess reactivity,

β = fraction of neutrons due to delayed emission from fission fragments,

ℓ^* = mean lifetime of prompt neutrons, and

$\lambda_i C_i$ = rate of neutron production from delayed neutron precursors, i, where λ_i decay constant of i^{th} precursor.

In order to solve this equation it is necessary to find a solution for the C_i's. For each precursor, C_i, a differential equation may be written:

$$\frac{dC_i}{dt} = \frac{\beta_i n}{\ell^*} - \lambda_i C_i . \qquad (2)$$

The term $\lambda_i C_i$ is the usual decay term for decay of a radioactivity source. β_i is the fraction of neutrons due to the i^{th} precursor and thus $\frac{\beta_i n}{\ell^*}$ is a source term for the i^{th} precursor.

At equilibrium in the reactor $\frac{dC_i}{dt} = 0 = \frac{\beta_i n}{\ell^*} - \lambda_i C_i$,

$$\frac{\beta_i n}{\ell^*} = \lambda_i C_i \quad ; \tag{3}$$

Also $\frac{dn}{dt} = 0$, thus

$$S + \frac{nk_{ex}}{\ell^*} - \sum_i \frac{n\beta_i}{\ell^*} + \sum_i \lambda_i C_i = 0 \quad . \tag{4}$$

Note that $\frac{\beta n}{\ell^*} = \frac{n}{\ell^*} \sum_i \beta_i$

and using equation 3 in equation 4,

$$-S = \frac{nk_{ex}}{\ell^*} \tag{5}$$

so that

$$k_{ex} = -\frac{S\ell^*}{n} \quad . \tag{6}$$

Since power is proportional to n, or P = bn, then at two different power levels,

$$k_{ex_1} - k_{ex_2} = bS\ell^* \left(\frac{1}{P_2} - \frac{1}{P_1}\right) \tag{7}$$

and it is seen that the excess reactivity necessary for equilibrium of the reactor is different at the two power levels and directly proportional to the source strength.

If a given radioactive sample is measured in the RMF at two power levels, and if the photoneutron production is important, a difference in the reactivity should be observed.‡ The magnitude of the change cannot be predicted unless ℓ^* and b are known, and S is determined. If sufficient measurements are made, then all three constants can be determined. In this experiment it was planned that only the effect should be detected, if it were possible. Thus the technique used to determine the effect of photoneutrons on reactivity measurements consisted of operating the RMF at two different power levels and comparing reactivities of the photoneutron-producing sample. The photoneutron-producing sample (BETT-51-8) used for this experiment originally contained 0.5 g of U^{235} and was selected because of its high gamma intensity and because of its large accumulated megawatt days. The sample was irradiated in the MTR for five hours at 40 Mw of continuous operation. After shutdown the sample was

‡ This technique was suggested by S. B. Gunst in private communication.

removed from the MTR, prepared for reactivity measurements, and inserted in various measuring positions of the RMF (Fig. 1). The gamma intensity was monitored at the servo chamber position with the use of a Victoreen "R" meter. Data were recorded as shown in Table I.

TABLE 1

GAMMA FIELD STRENGTHS AT SERVO CHAMBER POSITION

Sample	Time After Shutdown	RMF Position	"R" Meter
Bett-51-8	5 hr	1	646 r/hr
		3	1510 "
		4	5100 "
Bett-51-8	7 hr	1	603 "
		3	1410 "
		4	4740 "
Bett-51-8	55½ hr	1	246 "
		3	564 "
		4	1980 "

The servo chamber was electrically compensated with the sample in each of the measuring positions. The values of compensation voltage with the source located in Positions 3 and 1 were -38 and -23 v, respectively. Reactivity measurements were made at 10.0 w and repeated at a higher power level of 78.4 w (increasing power by approximately a factor of 8). In addition, reactivity measurements were repeated at the two power level settings with a constant compensation voltage of -38 v applied to the servo chamber. The reactivity values of the irradiated sample and an unirradiated sample are shown in Table II.

There appeared to be three sources of error present in the experiment which could result in the measurements of different reactivities at different reactor power levels, other than the photoneutron contribution. They are: 1) an uncompensated servo chamber for the changing gamma activity, 2) a moderator temperature change as a result of changing the reactor power level and upon the introduction of the sample into the RMF, and 3) the change in reactivity as a result of the fission product transient.

TABLE II

REACTIVITY COMPARISONS OF AN IRRADIATED AND UNIRRADIATED SAMPLE AT DIFFERENT REACTOR POWER LEVELS

Time After MTR Shutdown (hours)	Sample Identification	RMF Position	Net Reactivity $(\frac{\Delta k}{k} \times 10^{-4})$		Compensation Voltage (Neg. Volts)
			10 Watts	78 Watts	
8.5	D (unirradiated)	3	5.089		38
8.7	8 (irradiated)	3	2.544		38
9.3	D	1	5.696		23
9.3	8	1	4.767		23
9.8	D	1		5.714	23
10.0	8	1		4.774	23
10.3	D	3		5.102	38
10.5	8	3		2.506	38
10.8	D	1	5.739		38
11.0	D	3	5.115		38
11.2	8	1	4.793		38
11.3	8	3	2.534		38
11.8	D	1		5.712	38
12.0	D	3		5.102	38
12.3	8	1		4.796	38
12.5	8	3		2.538	38

In order to minimize these errors the servo chamber was properly compensated, sufficient time was allowed during changes in reactor power level to allow for temperature equilibrium in the moderator, and the reactivity measurements were taken during 8.5 - 12.5 hours after shutdown (Table II) of the MTR reactor during the peak of the xenon transient. It was felt that the last effect would be most noticeable, therefore the reactivity measurements were repeated after the peak of the xenon fission product 57 - 60 hours after reactor shutdown. At 57.5 hours after MTR shutdown the γ activity of the irradiated sample was again monitored with the use of the Victoreen "R" meter located at the servo chamber position (Table I). Compensation voltage was adjusted for null output current of the servo chamber and found to be -22 v with the sample in position 3 and -19 v in position 1. With the compensation voltage set at -19 v and with sample #8 in the RMF position #3, the output of the Keithly micromicroammeter read 9.0×10^{-11} amperes.

Reactivity measurements were again repeated for low and high reactor power settings. See Table III.

TABLE III

REACTIVITY COMPARISONS OF AN IRRADIATED AND UNIRRADIATED SAMPLE AT DIFFERENT REACTOR POWER LEVELS

Time After MTR Shutdown (hours)	Sample Identification	RMF Position	Net Reactivity ($\frac{\Delta k}{k} \times 10^{-4}$)		Compensation Voltage (Neg. Volts)
			10 Watts	78 Watts	
57.5	D (unirradiated)	1	5.692		19
57.7	D	3	5.082		19
58.0	8 (irradiated)	1	5.614		19
58.5	8	3	4.318		19
58.2	B (unirradiated)	1	3.917		19
58.3	B	3	3.258		19
58.6	D	1		5.738	19
58.8	D	3		5.097	19
59.0	8	1		5.619	19
59.2	8	3		4.308	19
59.3	B	3		3.933	19
59.5	B	1		3.285	19

The net reactivity values tabulated in Tables II and III are summarized in Table IV and are presented as the ratio of the unirradiated sample (D) to that of the irradiated sample (#8). It is shown that the ratios, for a low (10 watts) reactor power setting, compared to a high (78 watts) reactor power operation, are the same within the expected accuracy of reactivity measurements.

Photoneutron flux measurements were made following removal of the irradiated sample from the MTR. The sample was positioned in the center of the water hole lattice of the RMF and indium foils, 0.005 in. in thickness and one centimeter square were placed in the corner and at the side of the water hole lattice. The foils were attached to lucite which enabled them to be easily removed from the RMF. The foils were counted and gave indicated measurements of approximately 2×10^2 n/cm^2-sec for the foils in the corner water hole position and approximately 3×10^2 n/cm^2-sec. in the side position.

The net result of these measurements is that the photoneutron effect cannot be seen within the experimental error of the measurements. This is expected in view of the photoneutron flux level measured by foil activation. The flux level in the reactor at these powers is of the order of 10^8 n/cm^2-sec.

TABLE IV

SUMMARY OF REACTIVITY COMPARISONS OF AN IRRADIATED TO UNIRRADIATED SAMPLE RATIO (ρ_S/ρ_D)

Approx. Time After MTR Shutdown (Hours)	RMF Position	Compensation Voltage (Neg. Volts)	Ratio (ρ_S/ρ_D)	
			10 Watts	78 Watts
9.5	1	23	0.837	0.836
11.5	1	38	0.835	0.840
58	1	19	0.986	0.980
9	3	38	0.500	0.491
11.5	3	38	0.495	0.498
58.5	3	19	0.850	0.845

The fact that the source contributes only one millionth of this flux would suggest that the reactivity effect would be of the same order of magnitude, i.e., $\frac{\Delta k}{k}$ of the order of 10^{-6}. This small reactivity is at the limit of sensitivity of the reactor and in this case well within the scatter of the data points.

III. REACTIVITY EFFECTS DUE TO IMPERFECT COMPENSATION FOR GAMMA RADIATION IN THE SERVO CHAMBER

Rather significant errors in measurements of reactivity can exist upon the introduction of highly radioactive samples in the RMF. These errors can be attributed to the compensated ion chamber used to drive the regulating rod servo control system; this servo chamber, as it is called, responds to gamma rays emitted by the samples. Therefore, experiments were conducted to determine the magnitude of this error and its effect on reactivity measurements.

This experiment deals with the response of the electrically compensated ion chamber to changing gamma fields and its function as the control element of the RMF in the determination of reactivities associated with irradiated samples. In the RMF, reactivity measurements are made by reading the position of a regulating rod which has been calibrated in reactivity units. The regulating rod is controlled by a servo system such that a constant current is maintained in the servo chamber. If the servo chamber is properly compensated, the output current will consist of that current due solely to

the neutron flux. However, if the chamber is improperly compensated, the resulting current will have two components, one from the neutron flux and one from the gamma activity. This does not present a serious problem if the contribution due to gamma activity is constant, because all that will occur is a change in the power level, not a change in the criticality conditions. However, the measured reactivity of a sample having considerable gamma activity will be in error due to the decay of the gamma emitters. The decaying gamma field causes a varying contribution to the total servo chamber current. Therefore, the regulating rod position will be in error by an amount depending upon the magnitude and rate of change of the servo chamber current due to the decaying gamma emitters. The experiment described here is designed to measure the magnitude of this error.

An estimate of the reactivity effect due to a decaying gamma source can be calculated. The servo chamber output current is held constant by the action of the servo system. The regulating rod is adjusted by the servo such that the neutron flux is changed to keep the output current from the servo chamber constant regardless of the magnitude of the gamma current. This may be expressed as follows:

$$I = I_\gamma + I_n \tag{8}$$

where I is the total current from the chamber, I_γ is the net (or uncompensated) contribution due to the gamma field, and I_n is the contribution due to the neutron flux. The current from a decaying gamma source may be represented in terms of the decay constant of the gamma source λ, and the initial gamma current, $I_{\gamma o}$.

$$I_\gamma = -I_{\gamma o} e^{-\lambda t} \tag{9}$$

The minus sign indicates a current opposite to the neutron-induced current.

Because the neutron flux is changed to compensate for the gamma current, the neutron current may be expressed as

$$I_n = I_{no} + I_{\gamma o} e^{-\lambda t} \tag{10}$$

where I_{no} is the neutron current with no gamma field present. These currents are schematically represented in the sketch below.

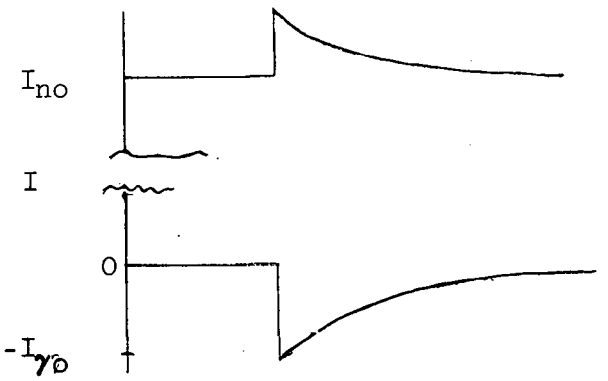

The basic assumption here is that the gamma emitter decays slowly compared to the response time of the servo and reactor system. At any time, the neutron flux is changing as shown in the sketch. Although the decay shown has an exponential form, the fact that the flux is not decaying toward zero eliminates a direct equating of the reactor period to the half-life of the gamma emitter. However, at any time the slope of the flux curve may be approximated by the initial slope of an exponential between that flux value and zero. In this way, an effective reactor period may be obtained and from this a quantitative measure of the reactivity.

An expression for the neutron flux if the reactor were on a true period is as follows:

$$I_n' = I_{no}' e^{-t/T} \tag{11}$$

where I_{no}' is the neutron current at the point where the slopes are to be equated, and T is the reactor period. The slope of the actual neutron current curve at the same point is

$$\frac{dI_n}{dt} = -\lambda I_\gamma \tag{12}$$

while the slope of a true period curve is

$$\frac{dI_n'}{dt} = -\frac{1}{T} I_n' \quad . \tag{13}$$

Equating the slopes at any given instant of time

$$\frac{-1}{T} I_n' = -\lambda I_\gamma \tag{14}$$

leads to a solution for the effective period, T:

$$T = \frac{I_n'}{\lambda I_\gamma} \quad . \tag{15}$$

I_n' is the neutron current at the time the slopes are equated, i.e.,

$$I_n' = I_{no} + I_\gamma \tag{16}$$

so that

$$T = \frac{1}{\lambda} \frac{I_{no}}{I_\gamma} + \frac{1}{\lambda} = \frac{1}{\lambda}\left(\frac{I_{no}}{I_\gamma} + 1\right) . \tag{17}$$

Note that $I_\gamma = I_{no} e^{-\lambda t}$ and if the compensation is at all adequate,

$\frac{I_{no}}{I_\gamma} \gg I$, so that for most cases

$$T = \frac{1}{\lambda} \frac{I_{no}}{I_{\gamma o}} e^{-\lambda t} \quad . \tag{18}$$

As an example, consider a case where $I_{no} = 100\ I_{\gamma o}$ and the emitter has a half-life of 54 minutes, i.e., I_n^{115}. Then,

$$\lambda = \frac{.693}{T_{1/2}} = 2.14 \times 10^{-4} \text{sec}^{-1}$$

and the reactor period T is

$$T = \frac{1}{2.14} \times 10^{+4}\ 100 \times 1 \text{ at } t = o$$

$$T = 4.67 \times 10^{5} \text{ sec.}$$

This period represents a reactivity of the order of $2 \times 10^{-7} \frac{\Delta k}{k}$.(2)

Should the compensation be only a tenth as good, the period would be 4.67×10^{4} sec, representing a reactivity of $2 \times 10^{-6} \frac{\Delta k}{k}$, and to compound this, for a 5 minute half-life emitter, the fastest which could be measured, the period would be 4.6×10^{3} sec or 20 μk.

Preliminary investigations were made to determine the magnitude of the total output current of the servo chamber due to gamma rays. The output current was measured under various conditions of compensating voltages and source locations to determine the dependence of the compensating voltage on gamma intensity and location of a test source.

The test source consisted of a piece of indium metal, approximately 2 g in weight, sealed in an aluminum capsule. Indium was selected because of its low energy gamma activity, (below the threshold energy of 2.2 Mev for deuterium), and because of its 54 minute half-life. The source was prepared by inserting it into the VH-2 rabbit facility of the MTR, (thermal flux of about 1×10^{14} nv), for exposure times of from three to five hours. The use of indium as a test source depends on the reaction:

$$In^{115} + n \rightarrow In^{116} \rightarrow Sn^{116} + e^-$$

In^{116} has two predominant gamma periods, one 13 seconds and the other 54.3 minutes. Since an elapsed time of approximately 15 minutes is required to transport the source from the MTR to the RMF, the short-lived activity is eliminated and only the 54.3 minute half-life activity remains. The energy of this gamma is below the threshold energy for deuterium. Thus no photoneutrons are produced by the gamma rays.

The calculated specific activity of the test source was 1.3×10^{14} disintegrations per second or 3,540 curies upon removal from the MTR. With the RMF shut down, the total output current of the servo chamber was measured by a Keithley micromicroammeter. The compensation voltage was adjusted for zero output current with the source positioned in each of the three RMF measuring positions (Fig. 1) and total output current recorded with the source moved to the other measuring positions. The data recorded are shown in Table V.

---

2. E. Fast, "Table of Reactivity Values for the RMF Calculated from the Inhour Equation," IDO-16361, 1956.

TABLE V

TOTAL OUTPUT CURRENT OF SERVO CHAMBER
FOR DIFFERENT SOURCE LOCATIONS
SOURCE INTENSITY -- 2,495 CURIES

Case	Source Position	Compensation Voltage (Neg. Volts)	Output of Servo Chamber	Compensation	Gamma Intensity at Servo Chamber
I	1	24.75	$<1.0 \times 10^{-13}$ amp	Total	600 r/hr
	3	24.75	$+2.5 \times 10^{-10}$	Under	1230
	4	24.75	$+2.2 \times 10^{-9}$	Under	3822
II	1	28.5	-1.0×10^{-10}	Over	600
	3	28.5	$<1.0 \times 10^{-13}$	Total	1230
	4	38.6	$+1.2 \times 10^{-9}$	Under	3822
III	1	41.75	-2.2×10^{-10}	Over	600
	3	41.75	-3.15×10^{-10}	Over	1230
	4	41.75	$<1.0 \times 10^{-13}$	Total	3822

The total output current of the servo chamber as a function of gamma ray intensity for Cases I, II and III is plotted in Figure 2.

Table V shows that as the location of the test source is changed, the total output current of the servo chamber also changes. This change indicates that the compensation voltage necessary for zero net output current is a function of the measuring position of the test source. In order to maintain compensation, the compensation voltage should be changed for each position of the test source and should also be varied as the activity of the test source changes.

The compensation voltage was adjusted for 28.5 volts, Case II, such that the servo chamber was compensated for Position 3. The total output current from the servo chamber was recorded for each position of the test source as the source decayed about nine half-lives. During this period of time, approximately 8 hours, the Keithley micromicroammeter was frequently checked for drifts. The total output current from the servo chamber as recorded by the Keithley was plotted (Fig. 3) as a function of time for the three RMF measuring positions. It is seen that with the test source in Position 4, the chamber becomes totally compensated about two half-lives later. The servo chamber then is over-compensated for all measuring positions.

A comparison was made of the magnitude of the total output current from the servo, with the chamber over-compensated, to the total output current of the servo with the RMF operating at normal power. The total output current as recorded by the micromicroammeter under normal operating conditions was 2.8×10^{-7} amps. Measurements of the servo chamber current made directly with and without the reactor at power, showed that the neutron current was a factor of about 10^3 above that of the gamma current. Using the results of equation 14, the reactivity effect expected is of the order of $10^{-8} \frac{\Delta k}{k}$, an entirely undetectable level.

The test source was again irradiated in the MTR to almost 100% saturation or about 3900 curies. A Victoreen type "R" meter was used to monitor the intensity of the gamma activity at the servo chamber position. The indium test source was placed in the three measuring positions of the RMF and the gamma intensity recorded at the start and termination of the experiment. The values recorded are listed in Table VI.

TABLE VI

GAMMA-RAY INTENSITIES OF In TEST SOURCE

Indium Source Position in RMF	Gamma Intensity (r/hr.)
1	900
3	1806
4	5220
No source (bkgnd)	80.4
(After 9 half-lives)	
1	99
3	111
4	148.2
No source (bkgnd)	85.2

The gamma activities measured with the use of the Victoreen "R" meter for the indium test source and for the BETT-51-8 sample are compared in the following table. It is seen that the gamma activity of the indium test source exceeded that of the most potent source (BETT-51-8) thus far measured in the RMF (Table VII).

TABLE VII

COMPARISON OF GAMMA-RAY INTENSITIES OF In TEST SOURCE

AND IRRADIATED FUEL SAMPLE

RMF Position of Source	Victoreen "R" Meter Readings (r/hr)		
	Indium Test Source		BETT-51-8
1	Exp. 1 600	Exp. 2 900	540
3	1230	1806	1260
4	3822	5220	4260

With the RMF critical and at normal operating power of about 10 watts, the regulating rod positions were recorded with the source located in the 3 RMF measuring positions. These positions were compared to the empty reactor regulating rod positions to determine the net reactivities. Measurements of reactivity continued for approximately 9 half-lives. Figure 4 is a plot of $\Delta\rho$ of the indium sample for RMF positions 1, 3, and 4 as a function of the number of half-life periods. It is seen that the deviation from the average is less than $\pm$ 2.5 μk^*, which is the normal error associated with reactivity measurements in the RMF.

Although the servo chamber was totally compensated at the start of measurements for source position 1, it appears that the largest $\Delta\rho$ was measured for this position. Source position 1, on the other hand, indicates the smallest $\Delta\rho$ over the 9 half-lives. For this position the servo chamber was over-compensated at all times. For these two source positions there is no indication that the $\Delta\rho$ has been in any one direction to indicate the influence of the decaying gamma field at the servo chamber. However, a slight $\Delta\rho$ in one direction is seen for source position 4. In this case, the servo chamber was under-compensated until the second half-life, as explained earlier in the report, after which the chamber became overcompensated as a result of the decrease in gamma ray intensity.

* $\mu k = 1 \times 10^{-6} \frac{\Delta k}{k}$

The magnitude of the decaying gamma-ray effect can be increased from the source strength decays such that the ion chamber passes from under-compensation to overcompensation. Although not subject to analytical treatment, a qualitative explanation is that the effective decay constant of the gamma current is increased as the gamma field passes through the compensation point on the chamber. Of course the ratio I_{no} to $I_{\gamma o}$ becomes infinite at compensation, but in this case the approximation that the servo system and reactor response is fast enough to follow the chamber is no longer valid. Except at this undefined region, the ratio I_{no} to $I_{\gamma o}$ is not variable by more than an order of magnitude while the decay constant could easily be magnified by an order of magnitude with the additional complication that the sign of the effect is changing.

This series of experiments confirms the prediction that the gamma-ray effect due to lack of compensation cannot be seen within the limits of observation. It is, however, possible that some of the scatter in the reactivity values is due to the changing compensation characteristics. The possible trend seen in the position 4 measurements could be the result of the gamma field strength decaying through the compensation point, but it is more likely to be a statistical effect.

As will be seen in the next section, the compensation voltage can be set such that a constant percentage of the gamma current is eliminated over several orders of magnitude of field strength. Although this compensation is not quite as good as can be obtained, the reactivity effect can be predicted with greater accuracy than if the percentage compensation is changing.

IV. COMPENSATED ION CHAMBER TESTS

In order that a type of compensated ion chamber could be selected for use in the RMF and ARMF, comparison was made between an electrically compensated chamber and a geometrically compensated chamber, i.e., a chamber in which the compensating geometry is fixed. The former is the Westinghouse Electric Company Mod. #WL6377 and the latter is the General Electric Company Mod. #5467870. Only one chamber of each type was available for testing so that the results of these comparisons cannot be applied with any degree of statistical accuracy.

Two criteria are used to judge the performance and usability of the chambers. The first criterion is the gamma compensation ability of the chamber; the second is a combination of the signal-to-noise ratio coupled with the absolute sensitivity of the chamber. In spite of the low flux (10^6 nv) in the RMF and the resulting low gamma field generated in the RMF, the gamma radiation encountered by the chamber can be as much as 10^5 r/hr when irradiated samples from the MTR are measured in the RMF. In order that the disturbance due to the gamma field be reduced to a minimum, the compensation of the chamber needs to be as nearly perfect as possible. The use of a compensated ion chamber as a detector for the servo system which drives the regulating rod makes a low-noise

chamber necessary. Since part of the noise is due to statistical fluctuations in the current, the more sensitive chamber is more desirable. Other sources of noise in the chambers would, of course, depend on the chamber type and also construction of the particular chamber under test. The description of the tests performed to determine which of the two types of chambers better suits this application are described in the sections which follow.

A. Gamma-ray Compensation Tests

Tests for compensation in a gamma-ray field were made in the Gamma Facility at the NRTS. The gamma field in this facility is produced by use of arrays of spent fuel elements from the MTR-ETR. For the measurements described here, gamma grid #2 was used. The gamma intensities at various positions on the grid are shown in Fig. 5. The intensities were measured at the horizontal plane passing through the center of the fuel elements.

Positions at which the chambers were tested are H-4, L-6, and L-16 on the grid, while a lower flux was obtained off the L-16 corner of the grid further away from the fuel. The cadmium-covered fuel boxes were used as positioning devices for the chamber dry hole. Fuel elements were stacked in a slab array along lines A through D extending from line 1 through 9. A thin-walled aluminum tube was used to keep the chambers dry during the tests. The gamma intensities quoted throughout this report were those measured with a Victoreen roentgen rate meter inserted into the dry tube at the chamber position. A vertical intensity distribution at position L-6 was taken with this instrument and is shown in Fig. 6. The vertical chamber position is indicated by the solid rectangle with the sensitive volume of the chambers shown by the horizontal marks. It will be noted that the intensity variation over the sensitive volume is about 10%, a condition not unlike that which is encountered in the Reactivity Measurement Facility. A semilog plot of the intensities along grid line 5 (Fig. 7) shows that the decrease in field strength is nearly exponential being a factor of 2 every four inches. Because the source arrangement approximates an infinite plane source, the decrease can be attributed to the attenuation in the water. When the dry tube is inserted into the field, the gradient across the diameter of the chamber is considerably lessened because of the lower attenuation in the air. The gradients of the gamma field in these tests are similar to those expected in an operating condition. However, it is expected that the gradients will be worse when radioactive samples are used in the RMF since they are more nearly point sources; this implies a greater than exponential fall-off in intensity as the distance to the source is increased.

Because of the lack of suitable facilities for establishing different gradients, no attempt was made during these tests to evaluate the importance of the gradients to the gamma response and compensating ability of the chambers. Because both types of chambers are essentially two concentric cylinders, both chambers should show the same characteristics under conditions of gradients in the gamma field.

The output current from the chambers was measured with a Keithly Model 410 micromicroammeter connected through 40' of RG-149/U low-noise coaxial cable to the signal connector on the chamber. A combination of battery and electronically-regulated power supplies was used to supply the appropriate voltages to the chambers. Type RG-62/U coax cable was used to carry the potentials from the power supplies to the chamber under test. The output of the micromicroammeter was connected to a Sanborn Model 60-1300 recorder. The recorder permitted noise traces to be taken when desired.

At each of four gamma-ray intensity levels, saturation characteristics were measured for the neutron sensitive portion of the chamber as well as for the compensating portion of the chamber. When the saturation characteristics of one part of the chamber were being measured, the power supply lead of the other part was connected to the common ground. The saturation curves are shown in Fig. 8. The electrically compensated (EC) chamber exhibits complete saturation of the gamma current in the neutron sensitive part of the chamber above 25 v for all levels of gamma field strength (Fig. 8b). The compensating volume of the chamber shows a very slight rise in current above the compensating voltage for all levels of radiation. This rise is expected of the chamber which is designed to permit overcompensating at all levels of gamma-ray intensities. The point of compensation is near enough to the quasi-level portion of the curve to prevent the amount of overcompensation from becoming unsafe from a reactor safety viewpoint. Safety considerations will be discussed later. The saturation characteristics of the geometrically compensated (GC) chamber (Fig. 8a) show the desired flat portion of the neutron sensitive section at all radiation levels. The curves for the compensating half of the chamber do not flatten out nearly as well as the EC chamber until 150 v are applied to the chamber above which point the response is flat for all levels of radiation. This property suggests that there is a possibility of finding a set of operating voltages which will provide exact compensation for the chamber. Electrical compensation can be achieved in the GC chamber as will be shown later. The horizontal bars indicating the current due to neutrons at a representative RMF power level show that the gamma current can greatly exceed the neutron current in that portion of the chamber. In order to measure the neutron current under these conditions, it is apparent that the compensation must be of the order of 1%. Even if this degree of compensation is achieved, there remains the question of the accuracy of any measurement made under conditions of large gamma-to-neutron current ratios.

The absolute sensitivity of the chambers to gamma rays may be compared. This is the current due to gamma rays only as measured at the flat part of the saturation curves. A comparison of the two chambers is shown in Fig. 9. It is seen that there is little difference between the two chambers.

At each of the four gamma-ray intensities the net output current from the chamber was measured as a function of the compensating voltage. In the case of the EC chamber, the curves all showed typical characteristics (Fig. 10a to 10d). At all levels the chamber was overcompensated

at or above 35 v. The current at "compensation" was erratic and noisy as indicated by the vertical bars on the graphs. In the undercompensated region, the rate of change of the output current as a function of the compensating voltage is quite high; above the compensation voltage the rate of change is considerably less. In each case, the error in compensation is of the order of 2% at 140 v, the error being in the direction of overcompensation.

From the point of view of reactor safety, it is necessary to determine the neutron flux level necessary to override the net gamma current in the overcompensated region. At 1200 r/min the gamma current is 35% of that of the neutron current at the normal reactor level of 10 watts. Therefore the reduction in indicated power level would be only 35%. This reduction is not desirable, but is certainly not an unsafe condition, especially since the case chosen is beyond reasonable expectations in that the compensation supply voltage can be easily provided with an upper limit, e.g., a 33 v battery.

From the data taken for the net current curves it is possible to calculate the ratio of the net current to the uncompensated current for different values of the compensation voltage and gamma intensities. A family of such curves is shown in Fig. 11; the net-to-uncompensated current ratios are plotted as a function of the gamma-ray intensity for different compensating voltages. From these curves a compensating voltage can be picked which will satisfy the conditions desired in the system of which the chamber is to be a part. For all gamma intensities, the best compensation can be achieved by using a compensating voltage of 30 to 35 v. Over the entire intensity range measured, the compensation would remain better than 99.4%. These data were taken for only one chamber, and should not be applied as a general rule without first accumulating more data on several chambers.

Similar net current vs compensation voltage curves were run for the GC chamber (Fig. 12a and 12g). It is seen that at low levels of gamma radiation the chamber can be overcompensated and exhibits much the same type of response as the EC chamber. However, in order that the chamber be compensated the proper voltage must be applied. At 1188 r/min, Fig. 12f and 12g, the chamber cannot be overcompensated by adjusting the B+ or the compensating voltage. For safety considerations, this is a better type of operation than if the chamber were overcompensated at these gamma levels.

Perhaps the best conclusion that can be drawn as a result of these studies is that neither chamber fulfills all the requirements of an ideal compensated ion chamber. Furthermore, it is true that these tests do not cover all conditions under which the chambers can be tested. Response as a function of the shape of the gamma field would be very interesting, although time consuming. Damage due to gamma radiation could be studied. However, for use in the RMF and ARMF these studies fairly well indicate the potentials and limitations of the chambers. Under normal operating conditions, the gamma field due to the fission gammas in the reactor is about 2 r/min in the servo-chamber

position. Expected gamma fields from radioactive sources being measured in the reactor are of the order of 2000 r/min or less. For a given set of voltages applied to either chamber it appears that over this region of gamma intensities the EC chamber can be compensated better than the GC chamber. In addition, at any given flux level, the EC chamber can be compensated an order of magnitude better by adjustment of the compensating voltage. These facts alone do not enable a choice to be made between the two types of chambers for use in the Reactivity Measurement Facility; tests of performance under the actual operating conditions found in the reactor are discussed in the following section.

B. Neutron Tests

Two series of neutron tests were made using the RMF as a neutron source. The first series of tests measured the neutron sensitivity as a function of the voltage applied to the neutron sensitive region of the chamber. These tests result in a measurement of the saturation characteristics for the chamber. The effect of the compensating voltage on the neutron sensitivity was also determined. The second series of tests measured the noise level in the chamber under conditions of neutron flux alone and with a gamma field in addition to the neutron flux.

The current measurements were made in the same manner as those in the gamma tests. Here again the Keithley micromicroammeter was used to measure the current and the voltages were supplied by the same power supplies as before.

The neutron flux in the region of the chamber was measured using indium-aluminum alloy wires attached to the chamber as shown in Fig. 13. A map of the flux distribution over the chamber region with the EC chamber inserted into the servo-chamber position is shown in Fig. 14; a rough azimuthal plot is shown in Fig. 15. The position of the chamber and the reference directions are illustrated in the drawing of the RMF core, Fig. 1. It was assumed that the vertical flux distribution for the two types of chambers was the same and only an azimuthal distribution was taken for the GC chamber at one vertical position. Because the sensitive volumes of the chambers are nearly identical, the non-uniformity of the vertical flux distribution is not expected to cause any significant errors.

Saturation curves for the two types of chambers are shown in Fig. 16. No significant difference in the shapes of the curves is seen. The fluxes listed on this drawing are the average values over the region 8" from the bottom of the chamber. The flatness of the plateaus indicates that only a few volts need be applied to the chambers to operate them satisfactorily in the RMF. In addition, no change in the current is noticed when the compensating voltage is changed. The only justification for operating at low potentials would be if the noise level were significantly reduced; this would occur only in an improperly operating system since the noise at these flux levels is predominantly generated by the statistics involved in the ion collection process.

The method for measuring the noise while in presence of a neutron flux is illustrated in the block diagram, Fig. 17. Bucking the DC component of the current is possible because of the apparent low impedance presented by the Keithley micromicroammeter. By effectively bucking the DC component of the chamber current with the external source, the deviations in the current can be measured directly with the Keithley micromicroammeter. The use of the Sanborn recorder permits preservation of the signal fluctuations, a sample of which is shown in Fig. 18. The determination of the signal noise from this trace is rather qualitative in that only estimates of the mean spread can be made. Nevertheless, the same method was applied to both types of chambers and the results are shown in Table VIII. The addition of a gamma field of the order of 100 r/min increased the noise level which is also shown in Table VIII. These noise measurements were done with the RMF at its usual power level of 10 w.

The indications from the sensitivity tests are that the neutron sensitivity of each chamber is the same if compared to the neutron flux measured at the surface of the chamber. The difference in the flux at the surface is ascribed to a depression caused by the chamber with most of the depression due to the boron coating in the chamber; thus, it is assumed that the difference in the flux at the chamber surface between the two chambers is due to a difference in the amount of boron used in the chamber coating. In the application of the chambers to the RMF the sensitivity needs to be as high as possible. For servo operation the chamber with the higher signal-to-noise ratio is more satisfactory; however, the measurement of the noise done in this experiment is rather crude and is not as conclusive as it might be. In both the gamma and neutron tests, the electrically compensated chamber performed better than the geometrically compensated chamber. As a result, electrically compensated ion chambers have been chosen for future use in the RMF.

TABLE VIII

SUMMARY OF NOISE MEASUREMENTS

Type	Neutron		Neutron+		Neutron + Gamma+	
	Signal	Flux*	Noise	Signal/Noise	Noise	Signal/Noise
G.E.	1.5×10^{-7} A	2.25×10^{6}	.861	1.74	.934	1.60
W.E.	2.35×10^{-7}	4.38×10^{6}	.915	2.57	1.125	2.09

* At 10 w

\+ Arbitrary units

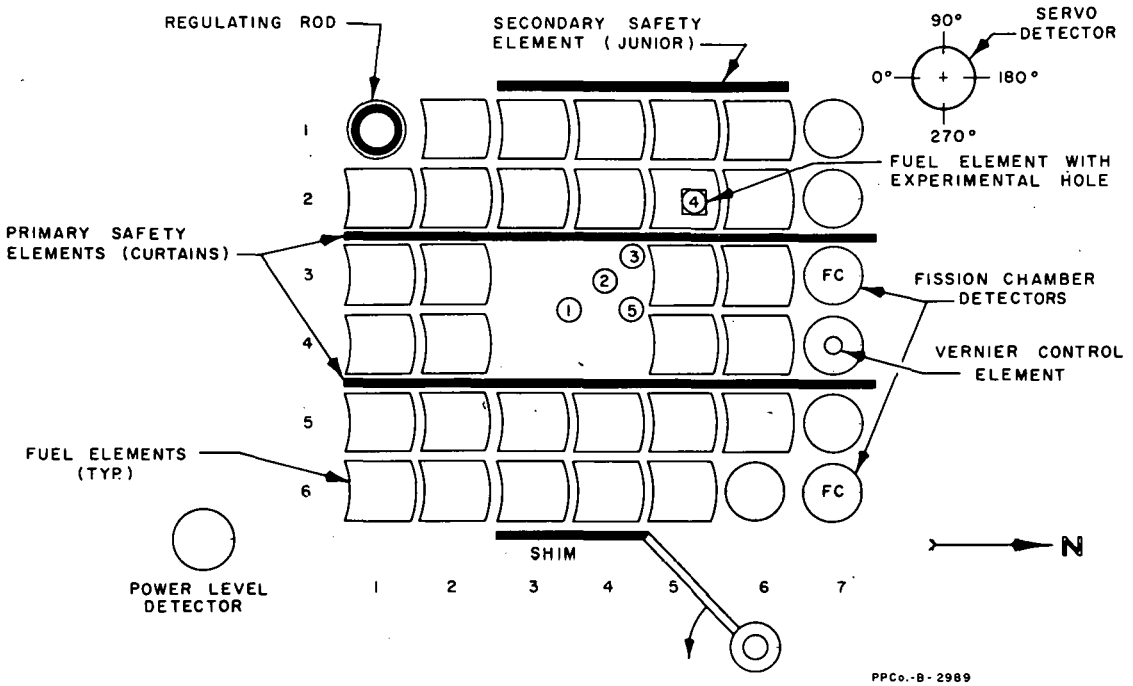

FIG. 1

SCHEMATIC OF RMF CORE

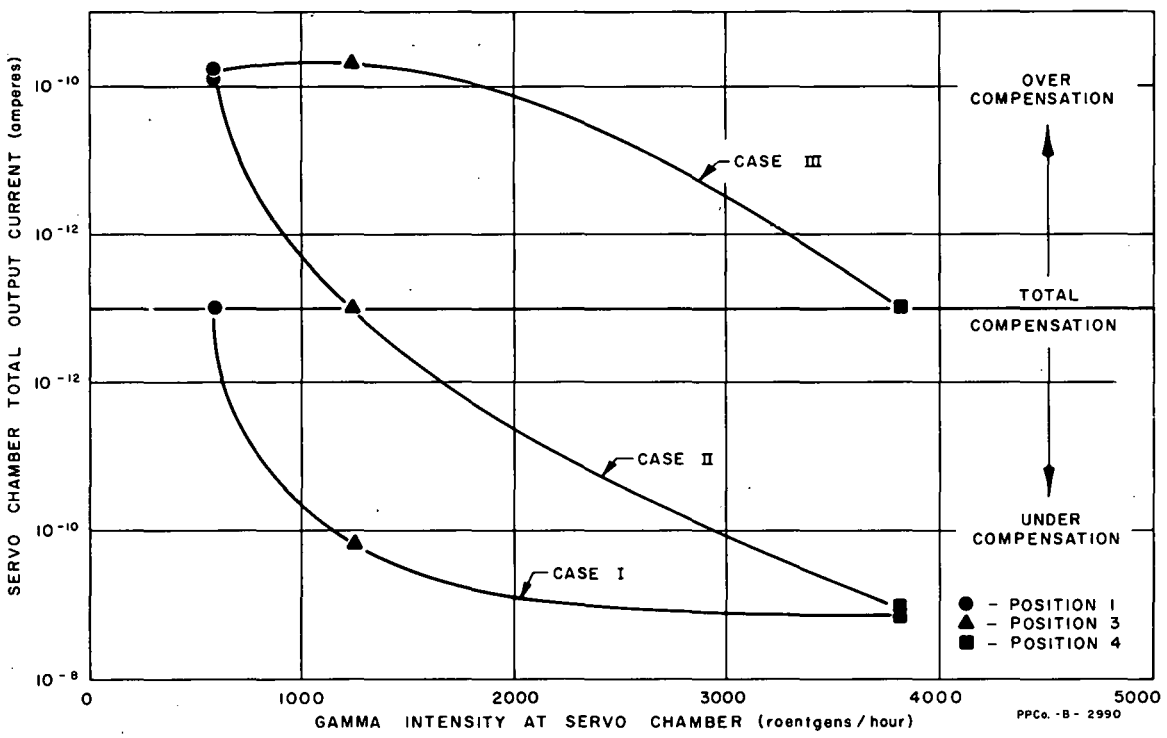

FIG. 2

SERVO CHAMBER TOTAL OUTPUT CURRENT vs.
GAMMA INTENSITY AT SERVO CHAMBER

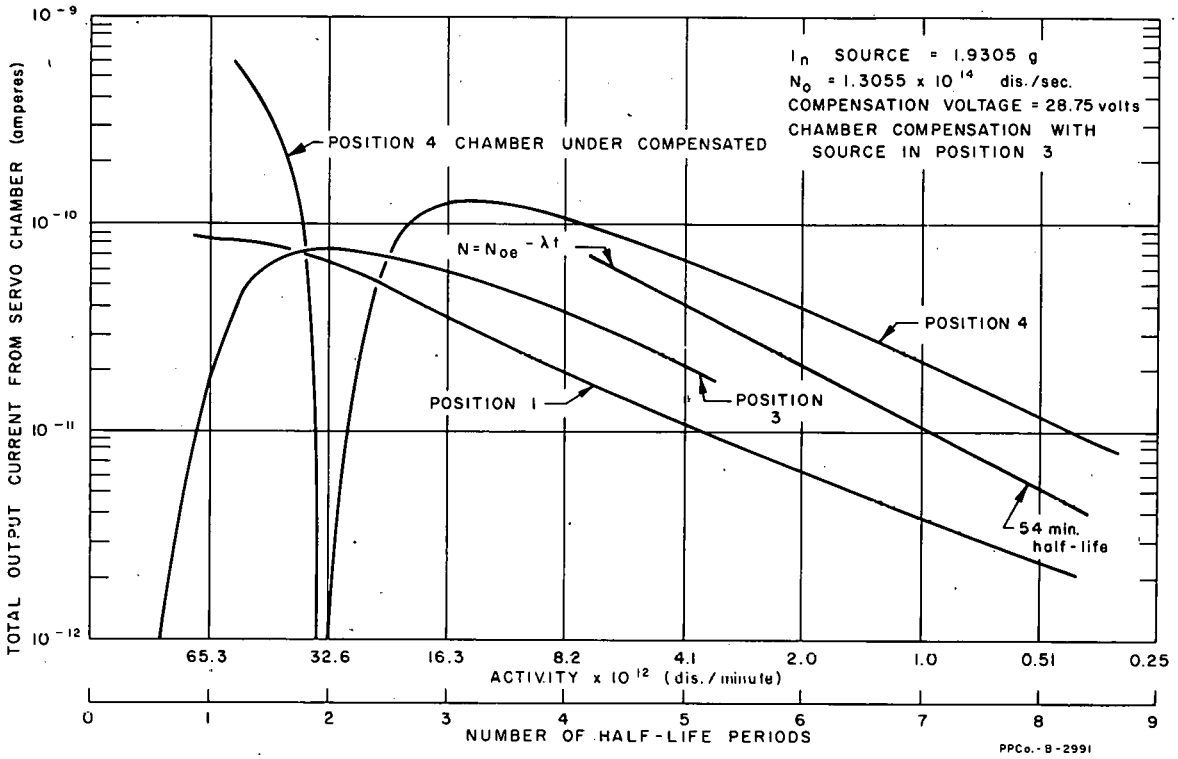

FIG. 3

TOTAL OUTPUT CURRENT FROM SERVO CHAMBER
vs. NUMBER OF HALF-LIFE PERIODS

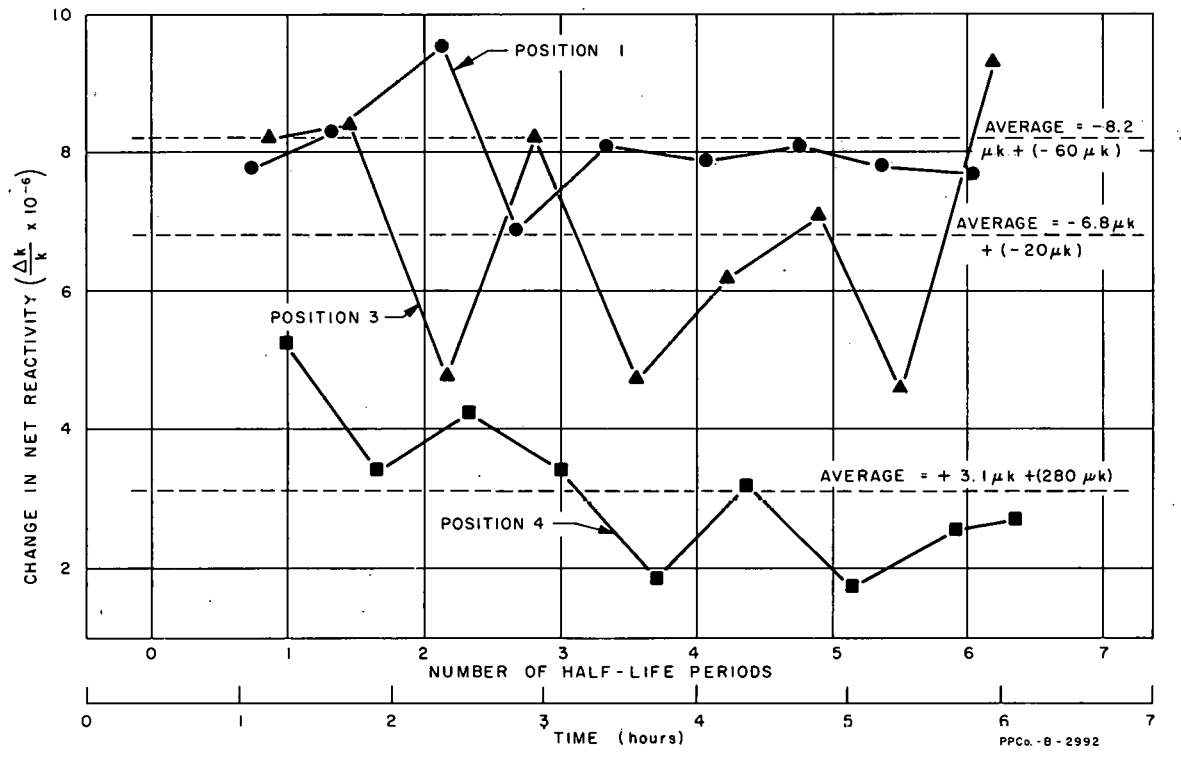

FIG. 4

CHANGE IN NET REACTIVITY vs. NUMBER OF HALF-LIFE PERIODS

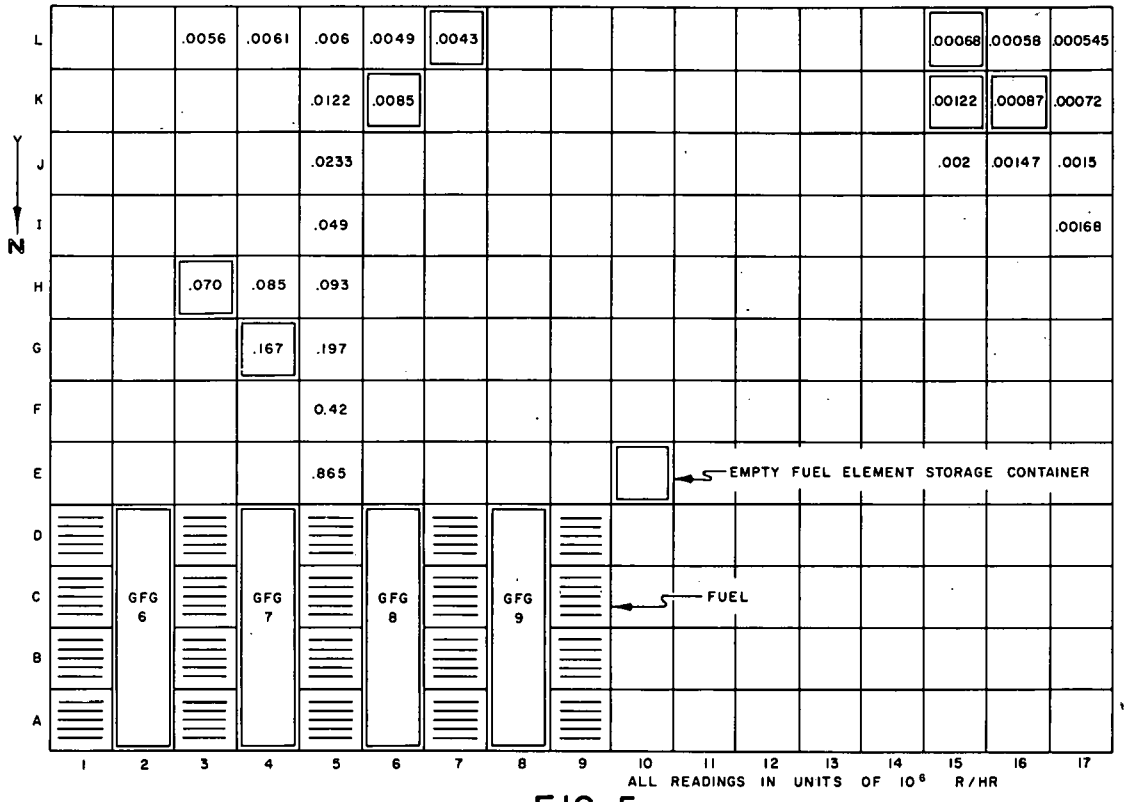

FIG. 5
INTENSITY MAP OF GAMMA GRID NO. 2

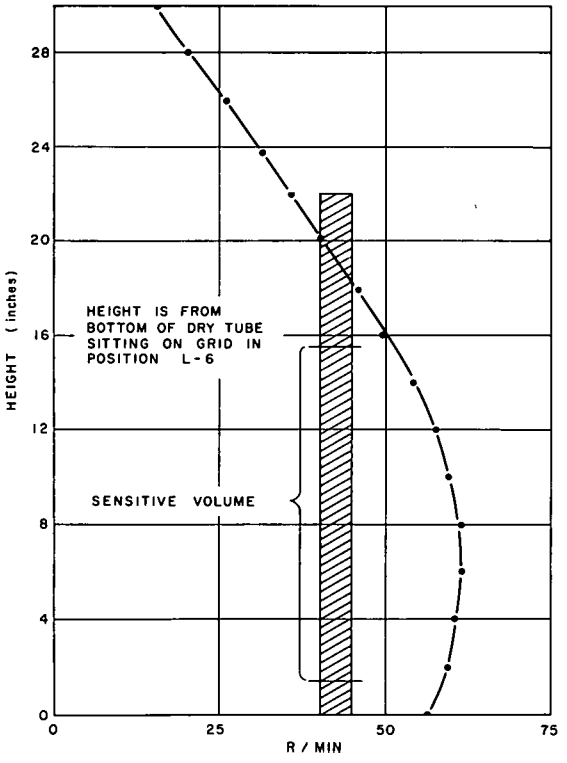

FIG. 6
GAMMA-RAY INTENSITY VERTICAL DISTRIBUTION

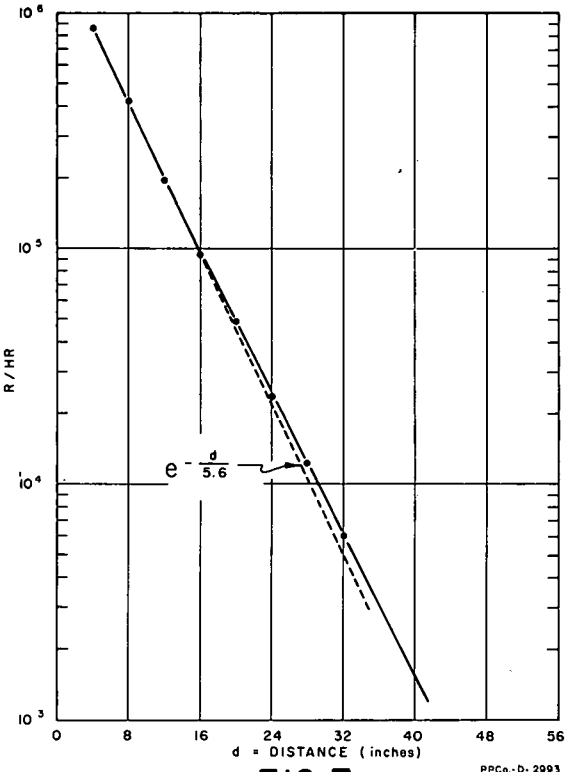

FIG. 7
GAMMA INTENSITY vs DISTANCE FROM FUEL (ALONG GRID LINE 5)

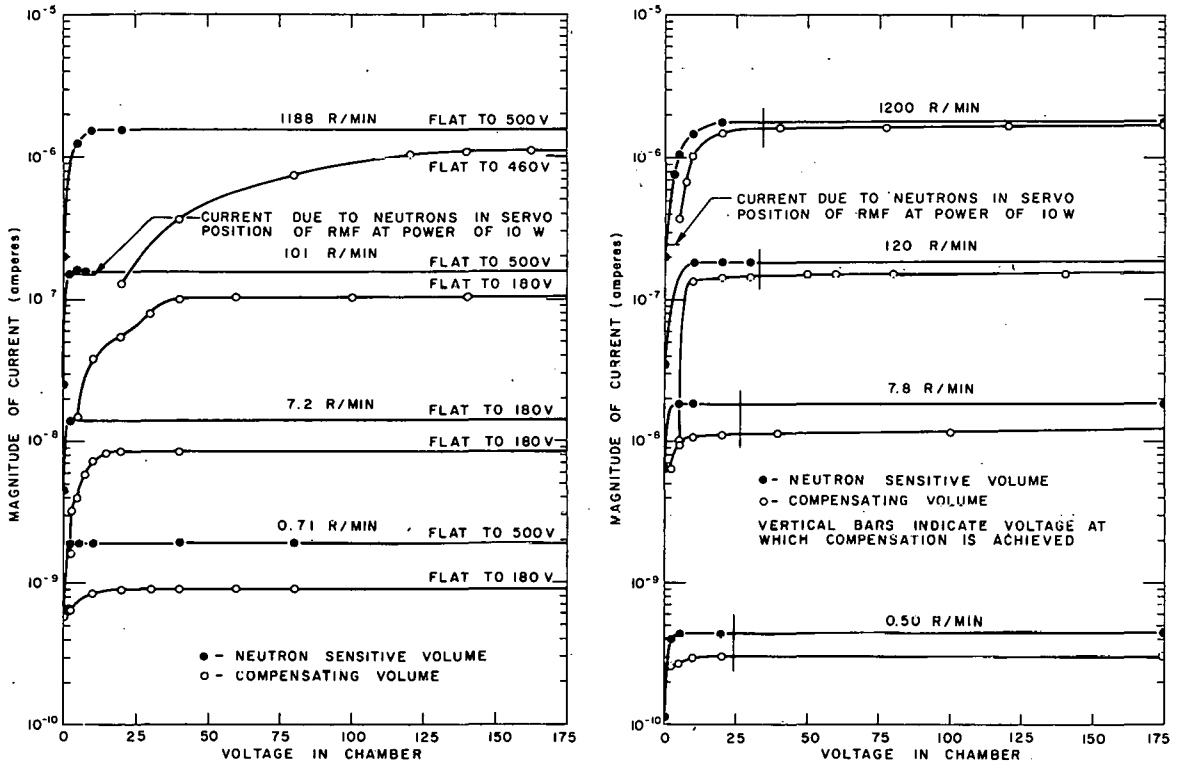

FIG. 8
SATURATION CURVES FOR GAMMA-RAYS

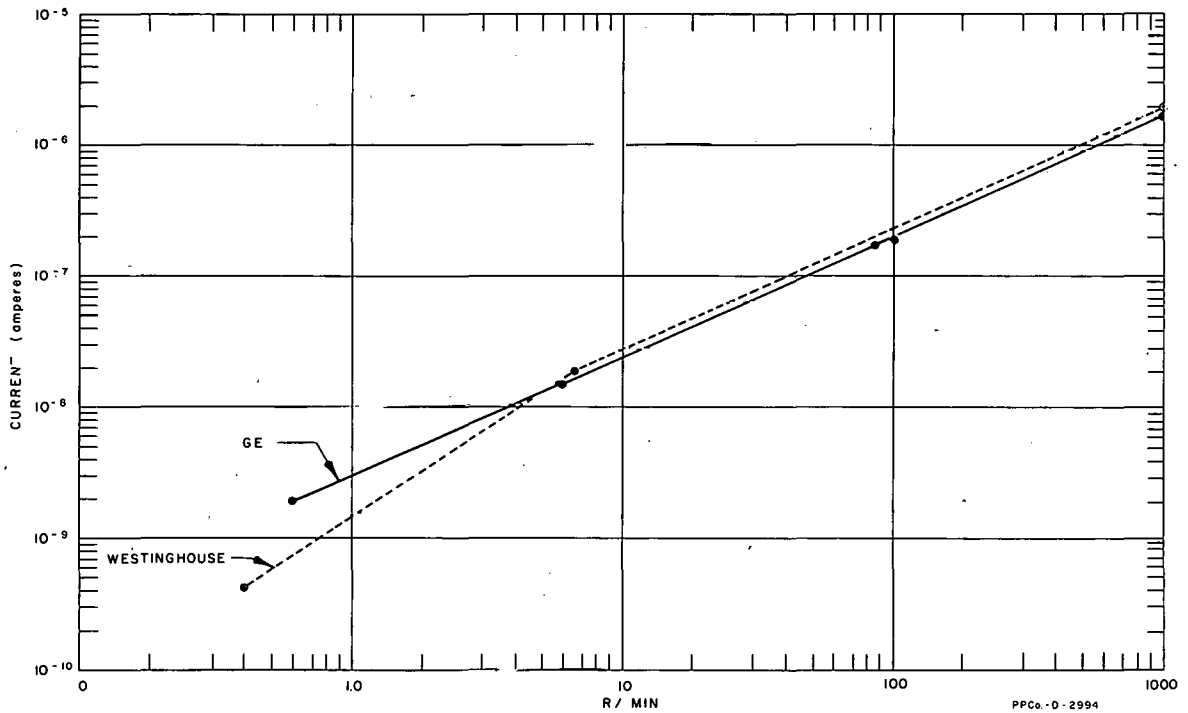

FIG. 9
CURRENTS FOR NEUTRON SENSITIVE VOLUMES ON FLAT PART OF PLATEAU IN A PURE GAMMA FIELD

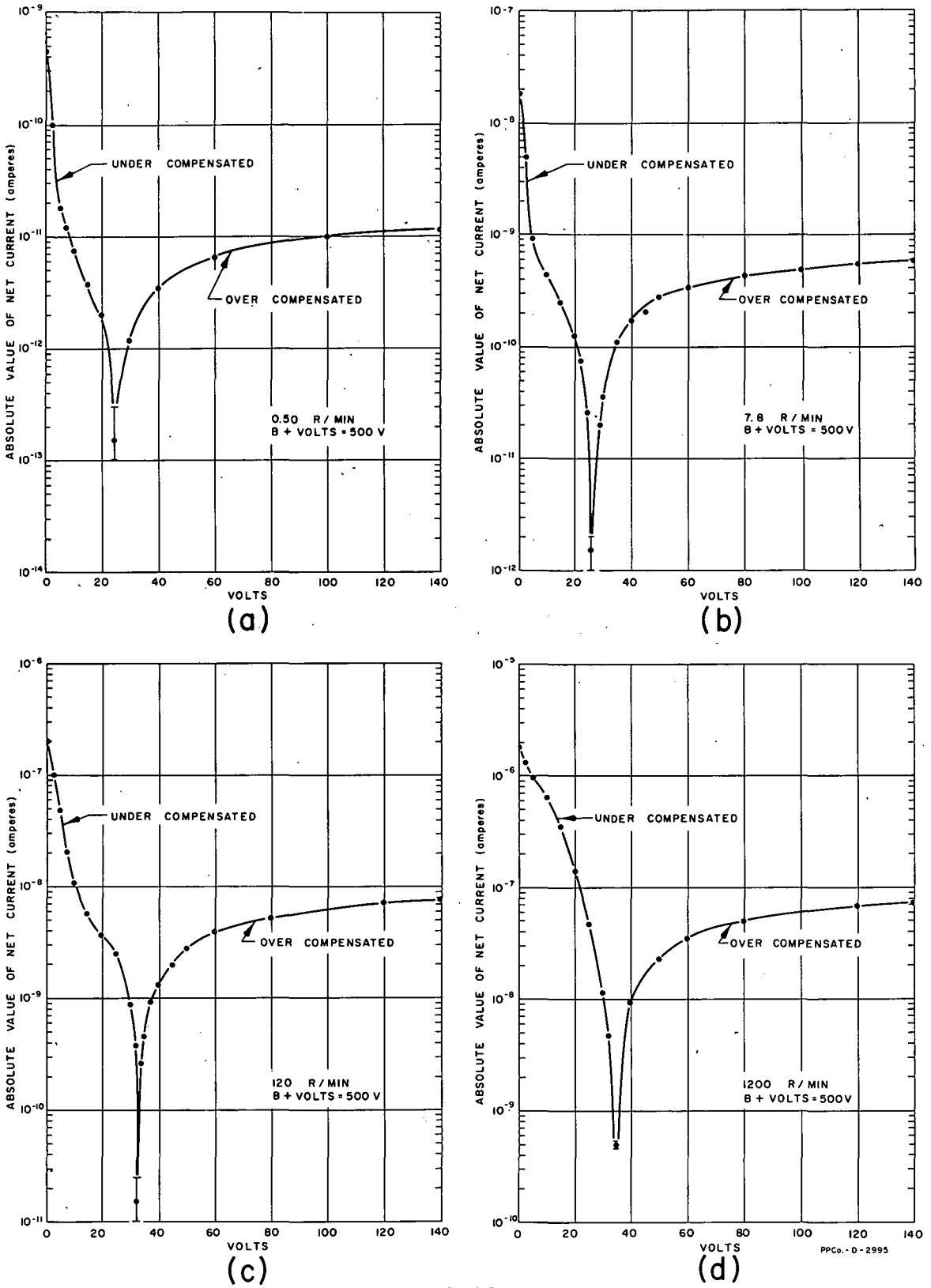

FIG. 10

NET CURRENT vs. COMPENSATION VOLTS FOR WESTINGHOUSE , CHAMBER, MODEL WL 6377, SERIAL NO. 93017

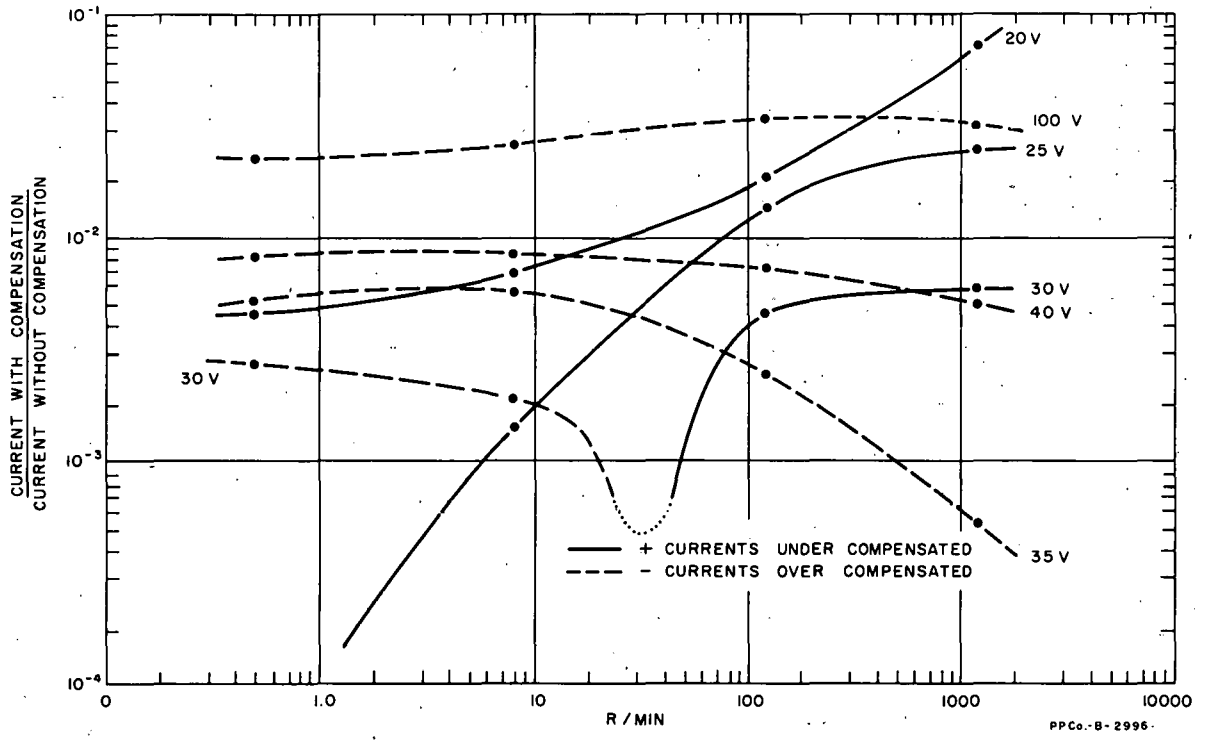

FIG. 11

COMPENSATION RATIO vs. GAMMA-RAY INTENSITY

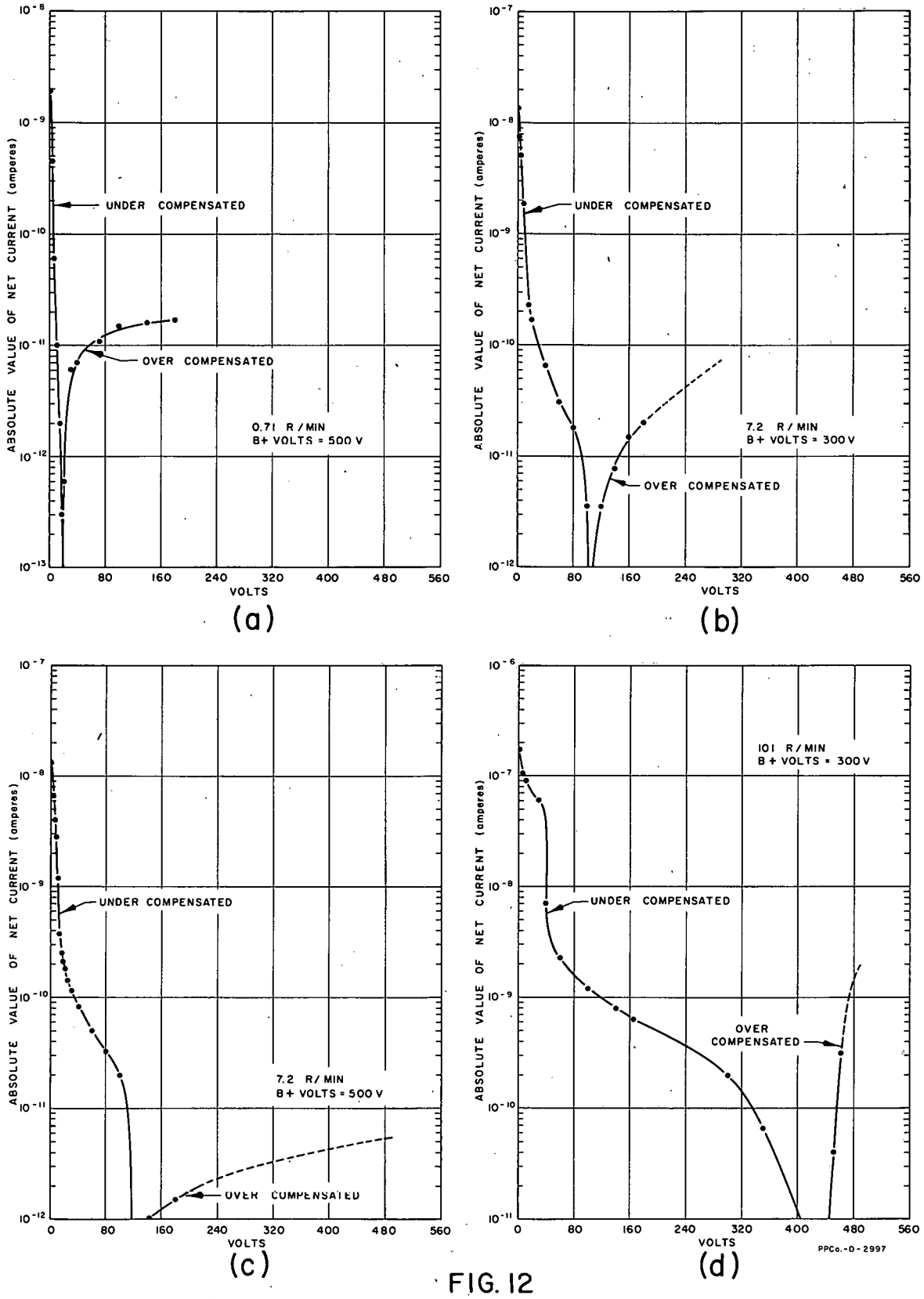

FIG. 12

NET CURRENT vs COMPENSATION VOLTS FOR GE CHAMBER
MODEL NO. 5467870, SERIAL NO. 4072956

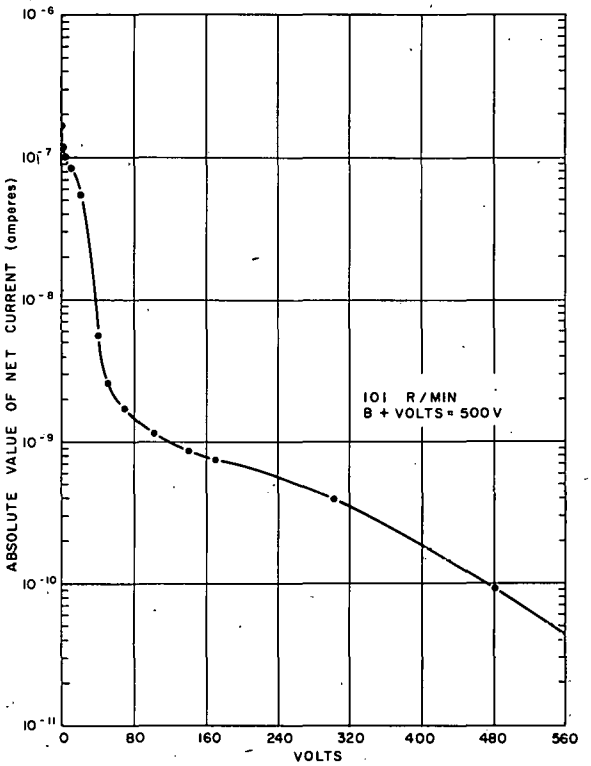

(e)

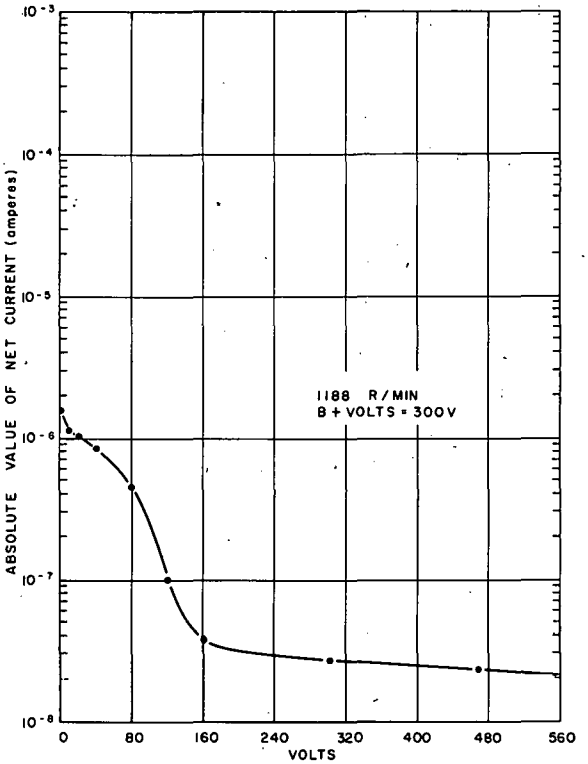

(f)

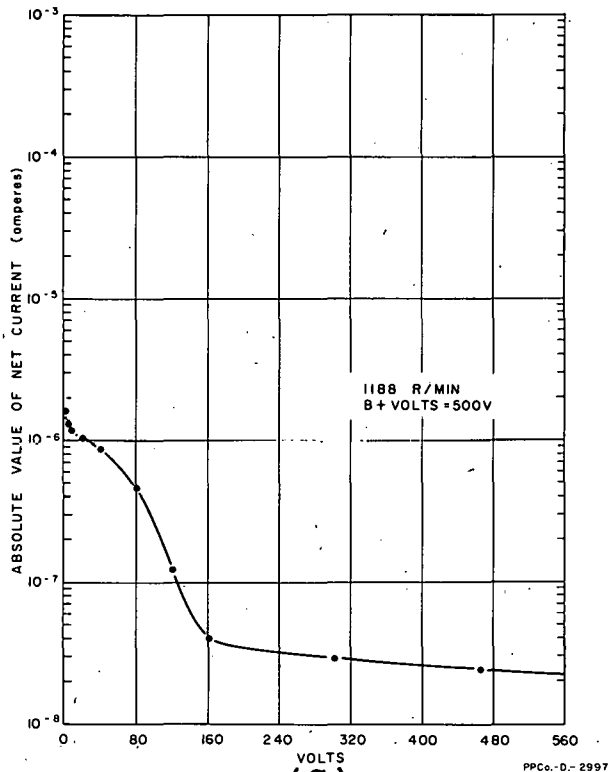

(g)

FIG. 12

NET CURRENT vs COMPENSATION VOLTS FOR GE CHAMBER MODEL NO. 5467870, SERIAL NO. 4072956

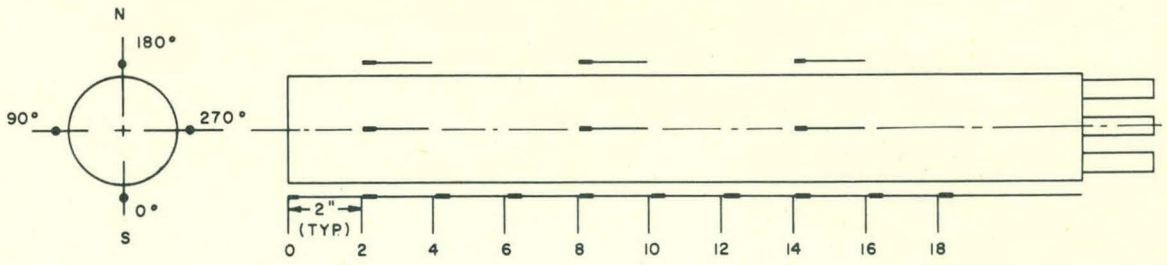

PPCo. - B - 2998

FIG. 13
POSITION OF FLUX WIRES ON CHAMBER

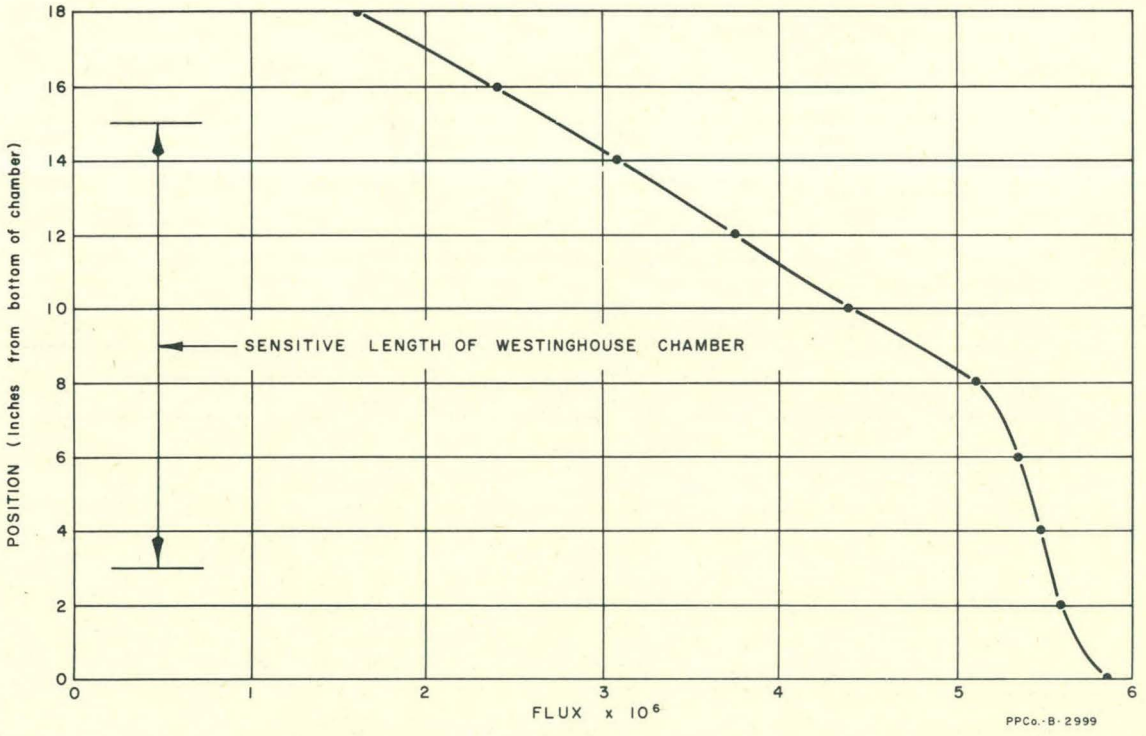

PPCo.-B-2999

FIG. 14
VERTICAL FLUX DISTRIBUTION IN SERVO CHAMBER POSITION

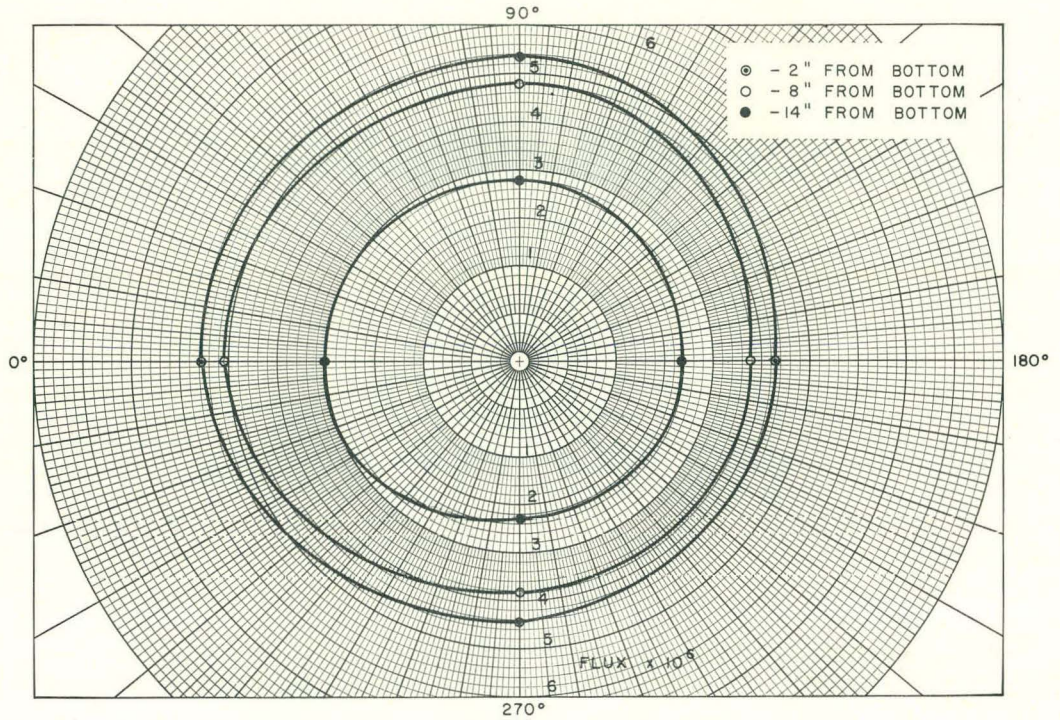

FIG. 15

AZIMUTHAL FLUX DISTRIBUTION IN SERVO CHAMBER POSITION

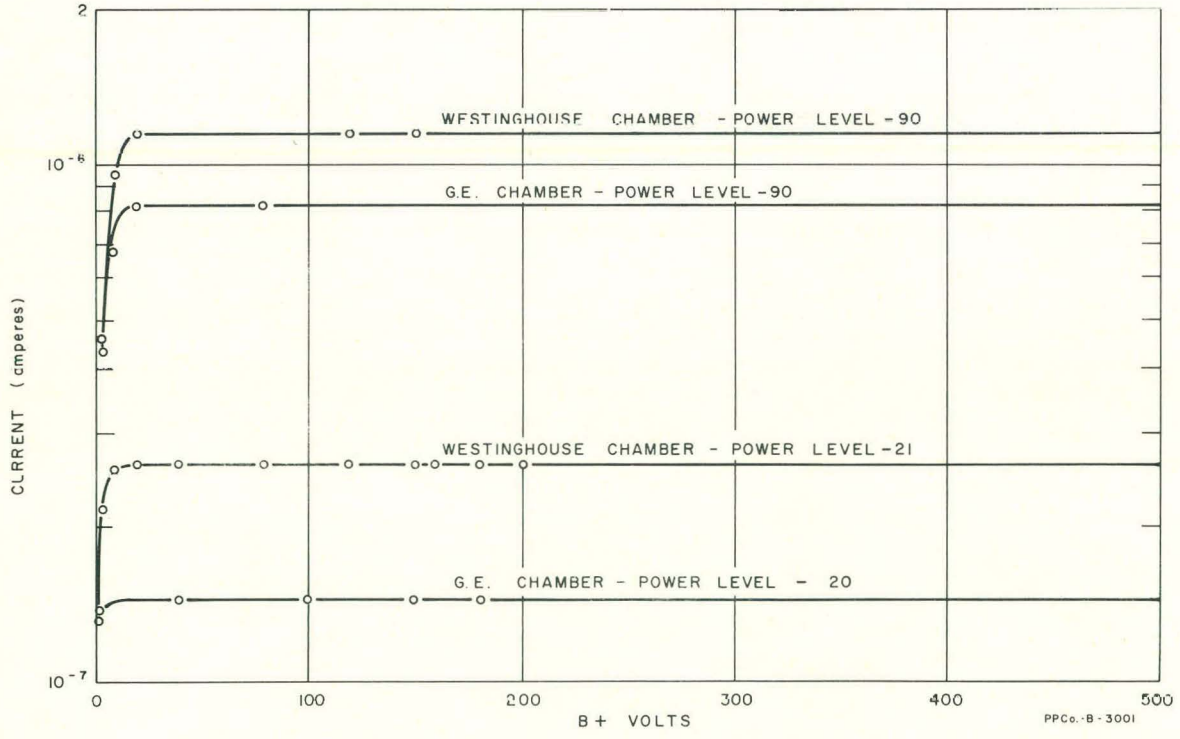

FIG. 16

SATURATION CHARACTERISTICS FOR NEUTRONS

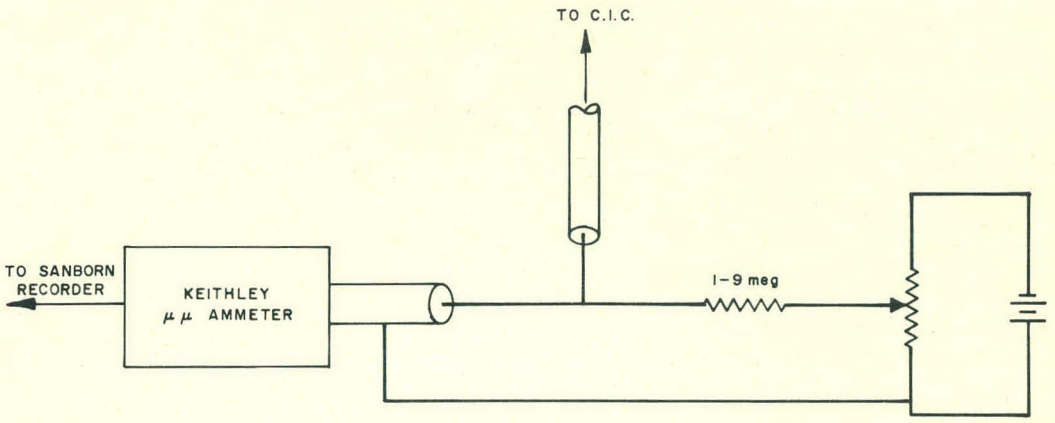

FIG. 17
BLOCK DIAGRAM FOR NOISE MEASUREMENT

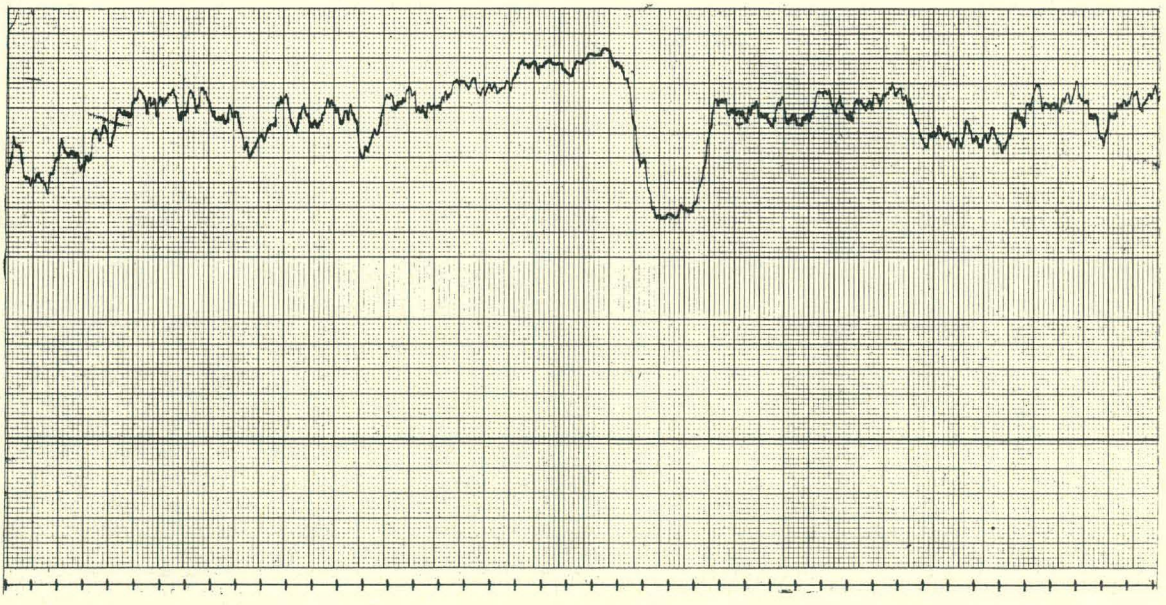

PPCo-B-3079

FIG. 18
SAMPLE NOISE TRACE

PHILLIPS
PETROLEUM
COMPANY

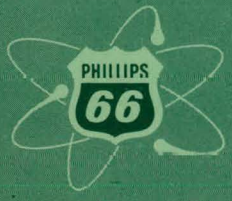

ATOMIC ENERGY DIVISION